Optik International Journal for Light and Electron Optics

White light reconstruction of a transparency registered in a BSO crystal

Myrian Tebaldi[1], María del Carmen Lasprilla A.[2], Néstor Bolognini[3]

Centro de Investigaciones Ópticas, CIOp (CONICET, CIC) and OPTIMO (Dpto. de Fisicomatemática, Facultad de Ingeniería, UNLP), P. O. Box 124, (1900), La Plata, Argentina

[1] Facultad de Ingeniería, Universidad Nacional de La Plata, Argentina
[2] Escuela de Física, Universidad Industrial de Santander, A. A. 678, Bucaramanga, Colombia
[3] Facultad de Ciencias Exactas, Universidad Nacional de La Plata, Argentina

Abstract: A monochromatic intensity distribution is encoded as modulation of the induced birefringence of a BSO crystal. In the read-out step, white light is employed and the birefringence modulation is transformed into a color modulation of the reconstructed image. The color associated to each point of the image at the output plane depends on both the birefringence modulation and the pass plane orientation of an analyzer. Experimental results are shown.

Key words: Birefringence – pseudocolored – BSO crystal

1. Introduction

Photorefractive crystals have been widely used in dynamic holography, light amplification, optical conjugation, optical signal processing [1, 2] and employed as spatial light modulators [3–6]. These materials are well suited for such applications because of their ability to encode light intensity distributions as a recyclable refractive index patterns. In particular, the sillenite photorefractive crystals (BSO, BGO, BTO) are fast and sensitive materials quite adequate for real time procedures.

The aim of this work is to analyze the color features of the image reconstructed by a white light source when an input transparency is stored in the photorefractive BSO crystal. The write-in monochromatic and spatially incoherent intensity distribution received by the crystal modulates its induced birefringence. As it is well known, the resulting elliptical birefringence depends on the crystal parameters (thickness, applied voltage, rotatory power) and the intensity distribution received. In the read-out step, white light is employed and the birefringence modulation is transformed into a color modulation of the reconstructed image. The color associated to each point at the output plane depends on both the birefringence modulation and the pass plane orientation of an analyzer. In the following sections the experimental set-up, the theoretical model and the experimental results are presented.

2. Description of the set-up and physical model

Let us consider the experimental arrangement of fig. 1. An input transparency T is illuminated by a white light source S_1 through the condenser lens L_1. An interference filter centered at the wavelength $\lambda_G = 530$ nm is placed in front of S_1. At this wavelength the BSO crystal exhibits a strong photoconductivity. The lens L_2 images the input transparency into the crystal. The directions $\langle\bar{1}10\rangle$, $\langle 001\rangle$ and $\langle 110\rangle$ of the crystal coincide with the laboratory axes *X, Y, Z* and its linear dimensions

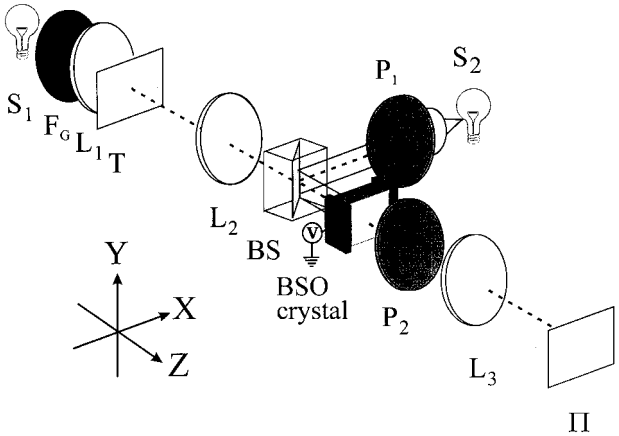

Fig. 1. Experimental set-up. S_1 and S_2: white light source, F_G: interferencial green filter; L_1: condenser lens; T: transparency; BS: beam splitter; P_1 and P_2: linear polarizers; L_2 and L_3: imaging lenses; Π: image plane.

Received 26 February 2001; accepted 10 June 2001.

Correspondence to: N. Bolognini
Fax: ++54-221-4712771
E-mail: Nestorb@odin-ciop-unlp.edu.ar

are L_X, L_Y and L_Z, respectively. Let us introduce the physical mechanism by which the input image is stored (write-in process). The crystal exhibits the linear electro-optic effect. It means that when a voltage V is applied between the (110) faces, which are separated each other a distance L_X, it becomes uniformly birefringent due to the external field $E_a = \frac{V}{L_X}$. The intensity distribution imaged onto the crystal creates photocharges that drift in the field E_a into the dark regions where they are trapped. These charges develop a space charge field E_{SC} that partially compensates the external field in the illuminated areas. The resulting space charge field gives rise to an electric field, which perturbates locally the refractive index via the electro-optic effect.

In the following we concentrate on a particular input to be stored. We consider that the intensity pattern received by the crystal is:

$$I_i(x) = I_0\left(\frac{1}{2} + \sum_{m=1}^{\infty} \frac{\sin(\pi m/2)}{\pi m/2} \cos\left(2\pi m \frac{x}{d}\right)\right) = I_0 \cdot t(x) \tag{1}$$

which represents a Ronchi grating of period d. Note that $t(x)$ is the normalized intensity distribution where x is the spatial variable. Then, to compute the total internal field E in the crystal a single spatial variable approach is employed [1, 7]. The generation rate of photocharges is proportional to the light pattern received by the crystal. Besides, diffusion of photocharges can be neglected because of the smoothed variation of the input intensity $I_i(x)$ in a microscopic scale, when considering the relative large period of the grating to be employed. Also, the photoinduced space charge field E_{SC} must fulfill:

$$\int_{-L_{x/2}}^{L_{x/2}} E_{SC}(x)\,\mathrm{d}x = 0 \tag{2}$$

where x is a spatial variable. Furthermore, in the steady state situation, a constant current density is of concern. The time required for these space charges to build up the field depends on the efficiency of the photoinduced charge transport. This transient stage requires few seconds under the conditions of our work. Afterwards, the steady state situation with a constant current density is reached. Under these assumptions the total internal field results [6]:

$$E(x) = \frac{V}{\left(\int_{-L_{x/2}}^{L_{x/2}} \frac{\mathrm{d}x}{N_D\left(1 + \tau \frac{g_0}{N_D} \frac{I_i(x)}{I_0}\right)}\right) N_D\left(1 + \tau \frac{g_0}{N_D} \frac{I_i(x)}{I_0}\right)} \tag{3}$$

where N_D is the density contribution of the free-charges in the dark, τ is the free-carrier lifetime, $I_i(x)$ the light pattern received by the crystal and $g_0 = \frac{\alpha \xi I_0}{h\nu}$ (where α is the intensity absorption, ξ is the quantum efficiency, $h\nu$ is the photon energy of the light and I_0 is the highest intensity value).

In our arrangement, the applied electric field direction coincides with the X-axis and the induced birefringence modulation δn results [6]:

$$\delta n(x) = n_0^3 r_{41} E(x) \tag{4}$$

where r_{41} is the electro-optic coefficient (we used $r_{41} = 3.42 \cdot 10^{-10}$ cm/V [8]) and n_0 is the refractive index at λ_G without applied field.

In the read-out process, polarized white light is employed. At the crystal output an analyzer P_2 is introduced and its pass-plane forms an angle β with respect to the X-axis. The BSO crystal exhibits rotatory power per unit length $\rho(\lambda)$ which combines with the induced birefringence modulation $\delta n(x)$. In this case, the Jones polarization transfer matrix is given by [9]:

$$W_C = \begin{pmatrix} \cos\Delta - \mathrm{i}\sin\psi \cdot \sin\Delta & -\cos\psi \cdot \sin\Delta \\ \cos\psi \cdot \sin\Delta & \cos\Delta + \mathrm{i}\sin\psi \cdot \sin\Delta \end{pmatrix} \tag{5}$$

where:

$$\begin{aligned} \Delta &= \Delta(x, V, \lambda) = L_Z \sqrt{\varrho(\lambda)^2 + \frac{\varphi^2(x,V)}{4}}; \\ \psi &= \psi(x, V, \lambda) = \tan^{-1}\left(\frac{\varphi(x,V,\lambda)}{2\varrho(\lambda)}\right); \\ \varphi(x, V, \lambda) &= \frac{2\pi}{\lambda}\,\delta n(x, V) = \frac{2\pi}{\lambda}\, n_0^3 r_{41} E(x, V) \end{aligned} \tag{6}$$

and L_Z is the crystal thickness and λ is wavelength of the read-out beam. The transfer matrix W_C is written in the induced axes X and Y which form an angle of 45° with the axes X and Y respectively. It should be emphasized that the rotatory power of the BSO crystal depends on the wavelength employed as shown in fig. 2 [10].

The matrix W_C governs the polarization transfer characteristics of the crystal by the relation:

$$\boldsymbol{A}^* = W_C \cdot \boldsymbol{A}^*_{\mathrm{in}} \tag{7}$$

where $\boldsymbol{A}^*_{\mathrm{in}}$, $\boldsymbol{A}$ are the polarization state vectors of light entering and exiting the crystal respectively. Both vectors are referred to the induced axes X' and Y'.

In our experimental conditions $\tau \frac{g_0}{N_D} \gg 1$. Besides, the crystal receives a stripe-like illumination. Under this assumptions and by taking into account eq. (6) the resulting internal field distributes itself periodically. In particular, in the bright striped areas the total internal field drops to a negligible value in comparison with the magnitude of the field in the dark regions where it increases beyond the external applied value E_a ($E \approx 2E_a$). As a consequence, the induced birefringence results:

$$\delta n(x, V) = \begin{cases} \delta n_1 = 0 & \text{if} \quad t(x) = 1 \\ \delta n_2 = 2 n_0^3 r_{41} \frac{V}{L_X} & \text{if} \quad t(x) = 0\,. \end{cases} \tag{8}$$

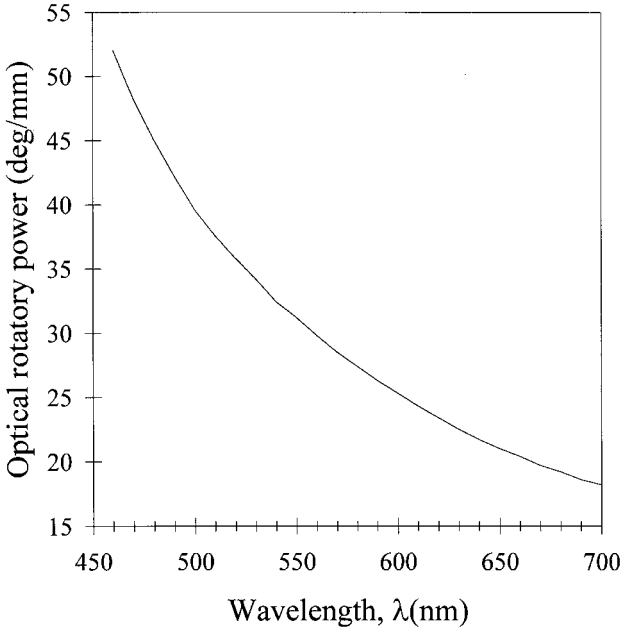

Fig. 2. Rotatory power of the BSO crystal as a function of the wavelength.

It is clear that the birefringence $\delta n(x)$ and the light pattern $I_i(x)$ have the same spatial period d. Therefore, the input transparency is registered in the crystal as modulation of birefringence.

Let us use vertically polarized light in the read-out process. Then, by taking into account eqs. (5), (6), (7) and (8), the resulting amplitude $\boldsymbol{A}(x, V, \lambda)$ that emerges from the crystal, referred to the laboratory axis (XYZ), can be expressed as:

$$\boldsymbol{A}(x,V,\lambda) = \left[\boldsymbol{A}^{(1)}(\lambda)\cdot t(x) + \boldsymbol{A}^{(2)}(V,\lambda)\cdot t\left(x-\frac{d}{2}\right)\right] \tag{9}$$

where $t(x)$ represents a Ronchi grating (see eq. (4)) and the amplitudes:

$$\boldsymbol{A}^{(1)}(\lambda) = \begin{pmatrix} A_X^{(1)}(\lambda) \\ A_Y^{(1)}(\lambda) \end{pmatrix} = \begin{pmatrix} -\sin\left(\varrho(\lambda)\, L_Z\right) \\ \cos\left(\varrho(\lambda)\, L_Z\right) \end{pmatrix} \tag{10}$$

and

$$\boldsymbol{A}^{(2)}(V,\lambda) = \begin{pmatrix} A_X^{(2)}(V,\lambda) \\ A_Y^{(2)}(V,\lambda) \end{pmatrix} = \begin{pmatrix} -\sin\Delta(V,\lambda)\cdot \mathrm{e}^{\mathrm{i}\psi(V,\lambda)} \\ \cos\Delta(V,\lambda) \end{pmatrix} \tag{11}$$

are associated to the write-in bright and dark regions of the crystal, respectively. By considering the resulting amplitude and the Jones matrix of the polarizer [10], the intensity distribution at the image plane emerging from the analyzer P_2 (see fig. 1) results [6]:

$$I(x,V,\lambda,\beta) = \left[I^{(1)}(\lambda,\beta)\cdot t(x) + I^{(2)}(V,\lambda,\beta)\cdot t\left(x-\frac{d}{2}\right)\right] \tag{12}$$

where:

$$I^{(1)}(\lambda,\beta) = \tfrac{1}{2}\left[1-\cos\left(2\varrho(\lambda)\, L_Z\right)\cdot\cos\left(2\beta\right) - \sin\left(2\varrho(\lambda)\, L_Z\right)\cdot\sin\left(2\beta\right)\right] \tag{13a}$$

$$I^{(2)}(V,\lambda,\beta) = \tfrac{1}{2}\left[1-\cos\left(2\Delta(V,\lambda)\right)\cdot\cos\left(2\beta\right) - \sin\left(2\Delta(V,\lambda)\right)\cdot\sin\left(2\beta\right)\cdot\cos\left(\psi(V,\lambda)\right)\right] \tag{13b}$$

where the angle β gives the orientation of the pass-plane of P_2 with respect to the X-axis.

It is clear that the output intensity depends on the read-out wavelength. That is, at each point, each spectral component of the white light source emerges from the crystal with a determined ellipticity. Therefore, the light passing through the analyzer will exhibit a maximum at the wavelength component whose polarization state is better transmitted by the analyzer. An examination of eqs. (13a) and (13b) reveals that the spectral behavior in the bright regions is different from that in the dark regions. In our calculations a rotatory power versus wavelength dependence as depicted in fig. 2 is employed. Also, we consider a BSO crystal of dimensions $L_X = L_Y = 10$ mm and $L_Z = 6$ mm and an applied voltage $V = 8$ kV. These values correspond with those of the experimental procedures.

Those parts of the read-out beam passing through the crystal regions where $\delta n_1 = 0$, have a spectral dependence for two selected orientations of the analyzer pass-plane as depicted in fig. 3a). These curves are obtained by using eq. (13a) ($I^{(1)}$) that corresponds to the bright regions of the input grating. Besides, the spectral behavior of the dark regions (fig. 3b)) is obtained by using eq. (13b) ($I^{(2)}$).

In fig. 3a) and 3b), the dashed and solid curves are calculated by using $\beta = 30^\circ$ and $\beta = 120^\circ$, respectively. Note that the dashed curve of the illuminated region in the write-in process is centered at $\lambda = 650$ nm and the dashed curve of the dark region is centered at $\lambda = 505$ nm. By the other hand, the solid curve ($\beta = 120^\circ$) of fig. 3a) is centered at $\lambda = 610$ nm while the dashed curve of fig. 3b) is centered at $\lambda = 530$ nm. That is, at these particular values of β the reconstructed images invert their colors. It is clear that by changing the value of β, the spectral region corresponding to the bright and dark areas will change accordingly.

In summary, the imaged input grating generates in the crystal a stripe-like birefringence distribution associated with the amplitudes $\boldsymbol{A}^{(1)}$ and $\boldsymbol{A}^{(2)}$ that in turn brings a colored transmitted beam when the white read-out light emerges from the crystal. It is clear that the pseudocolor reconstructed grating has the same spatial period d as the input transparency.

The absorption of the crystal depends on various parameters like purity, strain free nature, etc. The absorbance of the BSO crystal employed in our experiment is measured by using a spectrophotometer Beckman DU60 that operates between 200 nm and 900 nm.

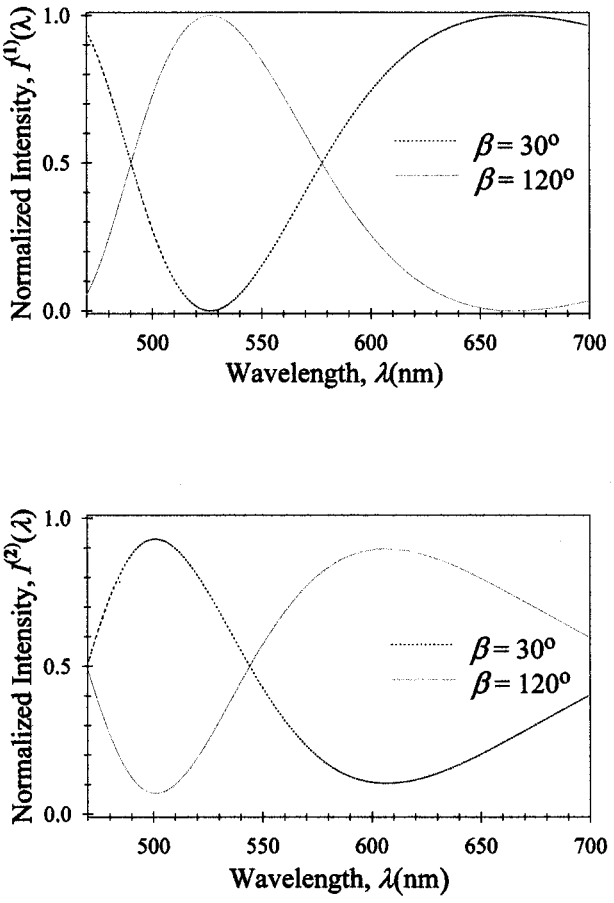

Fig. 3. Theoretical curves of the spectral dependence of the read-out beam passing through the crystal for two orientations of the analyzer pass-plane $\beta = 30^\circ$ and $\beta = 120^\circ$ and for: a) bright regions of the input grating b) dark regions of the input grating.

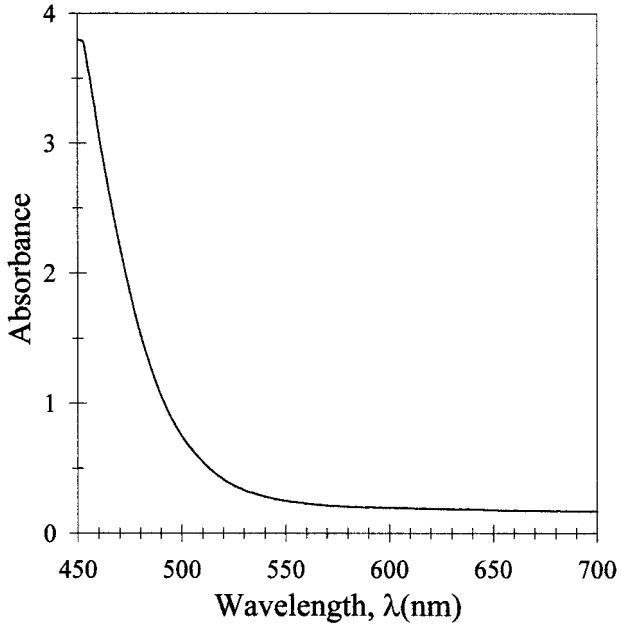

Fig. 4. Absorbance of the BSO crystal employed in our experimental arrangement.

The curve is shown in fig. 4 and it is apparent that $\alpha_{470\,\mathrm{nm}}$ is 100 times $\alpha_{>530\,\mathrm{nm}}$. Besides, an spectral range between 470 nm and 700 nm is considered in the theoretical curves shown in fig. 3.

On this basis, in many applications two different wavelengths λ_G (for instance 514 nm) and λ_R (for instance 633 nm) are employed, providing that the optical absorption (α) of the crystal behaves so that $\alpha(\lambda_G) \gg \alpha(\lambda_R)$. The photorefractive process at the wavelength λ_R is negligible in comparison with the photorefractive response at λ_G. Then, the wavelength λ_G induces a refractive index perturbation and this information can read-out by employing the wavelength λ_R without introducing significant changes.

It means that in our case a broad band read-out source of bandwidth 530 nm–700 nm should be employed otherwise the encoded birefringence modulation that stores the input could be erased. Nevertheless, such source could limit the performance of the processor because the blue-green region is missed. To avoid this situation a low power white light source for the read-out process is utilized. Also, mechanical chopper is used to alternate the write-in and the read-out process keeping the stored signal at a steady level. Moreover, this device avoids the superposition of both sources and to alter the pseudocolor hue values of the final image.

Experiments are carried out to verify the theoretical analysis. The reconstructed grating for two orientation of the analyzer is shown in fig. 5. In the experiments, a BSO crystal of dimensions $L_X = L_Y = 10$ mm and $L_Z = 6$ mm is used and a voltage $V = 8$ kV is applied in the (110) faces of the crystal. At the write-in and read-out processes a spatially incoherent white light source is used. A green interference filter is located at the output of the source in the write-in step. A lens L_3 forms an image of the crystal at the output plane (Π plane) and the encoded input is converted in intensity transmission by means of an analyzer P_2. There, a pseudocoloring version of the transparency as depicted in fig. 5a) and 5b) is displayed. The input transparency is black and white and two colors can be distinguished at the output. The induced birefringence depends on the write in illumination and the applied voltage through the space charge field. Then, the reconstructed color depends on the mentioned parameters and the analyzer orientations which coincide in fig. 5a) and 5b) with the corresponding orientations employed in the curves of fig. 3. Then, by comparing the theoretical analysis and the experimental results, it is apparently a good agreement in the resulting colors corresponding to the illuminated and dark write-in region.

As stated above, by rotating the analyzer it is possible to control the color of the output image. To show this feature, in fig. 6 is displayed the reconstructed im-

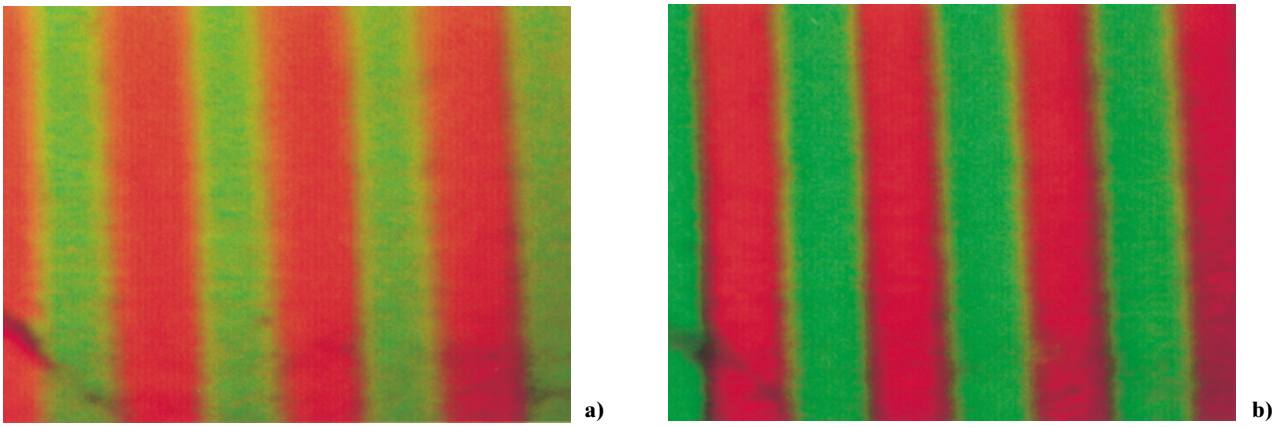

a) b)

Fig. 5. Reconstructed grating for the orientation of the analyzer P_2 given in fig. 3, $\beta = 30^\circ$ and $\beta = 120^\circ$.

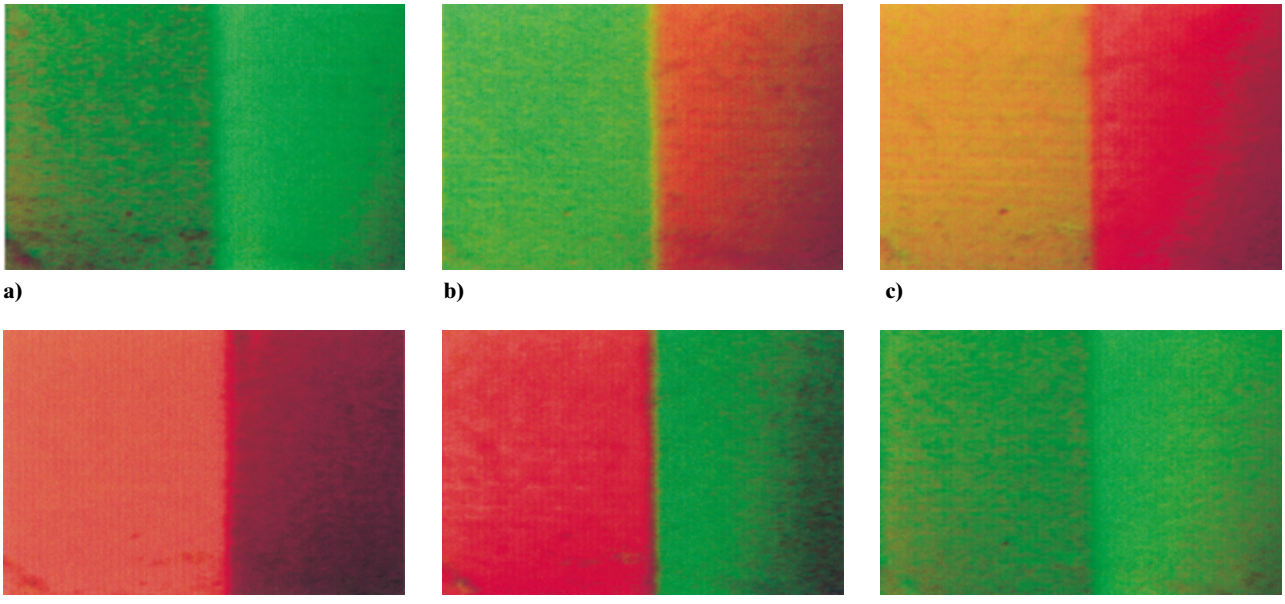

a) b) c)

d) e) f)

Fig. 6. Reconstructed images for six orientations of the analyzer P_2.

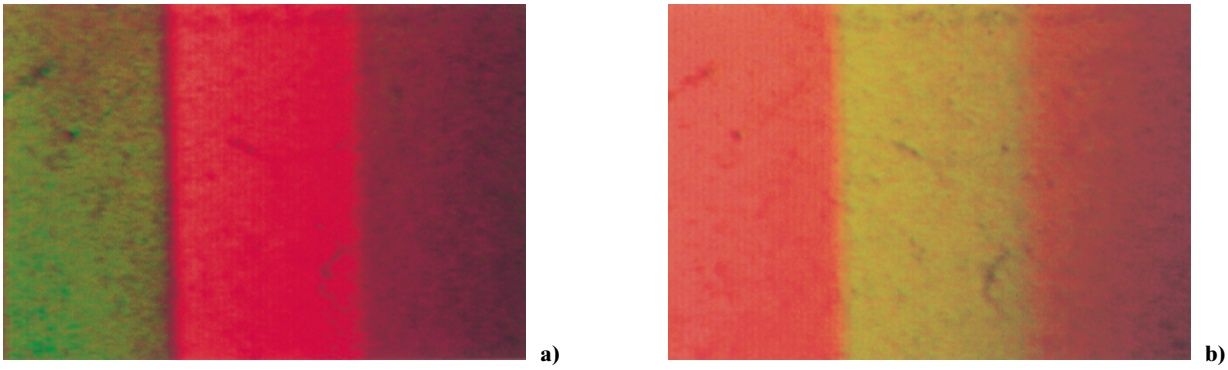

a) b)

Fig. 7. Reconstructed images of the transparency consisting of a sequence of three parallel fringes with different gray levels.

age for six orientations of the analyzer. In fig. 6f) the pass plane of the analyzer has been rotated 180° related to fig. 6a).

Note that in the cases detailed above the transparencies are bipolar (black and white) and therefore the crystal has two birefringence values. Nevertheless, our analysis can be extended to gray level images. In this case, it will result several birefringence values each one associated to the write-in gray level. In fig. 7 is displayed a pseudocolored image of a transparency consisting of a sequence of three parallel fringes with different gray levels. Each color corresponds to a determined gray level for a fixed analyzer orientation.

3. Conclusion

As it is well known the pseudocoloring of gray level information is a technique of introducing false colors into a black and white image. A new approach that employs a photorefractive crystal for pseudocoloring operations is proposed. A monochromatic spatial incoherent input is stored in the crystal as modulation of the induced birefringence. Therefore each birefringence value is associated to a determined gray level input. In the case of a binary image, the birefringence encoding produces two color states when is read out with polarized white light. Moreover, by using a gray level transparency, it will result several birefringence values each one associated to a determined write-in gray level. Taking into account that the induced birefringence depends on the write-in intensity distribution and the applied voltage through the space charge field, a suitable combination of these parameters and the analyzer orientation is necessary to obtain a prescribed color at the output. The theoretical analysis agrees with the experimental results as can be observed from fig. 3 and fig. 5. It should be mentioned that, the write-in and read-out process are simultaneously carried out within response times suitable to utilize the system as a real time optical processor. Notice that this arrangement depicts the input transparency by coding it in false colors without using spatial filters.

Finally, this pseudocolor method could be useful to analyze the local birefringence generated in the crystal through the color reconstructed.

Acknowledgement. This research was performed under the auspicious of the CONICET, Facultad de Ingeniería, U.N.L.P. (Argentina). M. Tebaldi acknowledges to CICPBA (Argentina). M. C. Lasprilla acknowledges MON (Multipurpose Optical Network).

References

[1] Yeh P: Introduction to Photorefractive Nonlinear Optics. John Wiley & Sons, New York 1993
[2] Huignard JP, Günter P: Optical processing using wave mixing in photorefractive materials. In Günter P, Huignard JP: Photorefractive materials and their applications II. Chapt. 6. Springer Verlag, Berlin 1989
[3] Marrakchi A, Tanguay Jr. AR, Yu J, Psaltis D: Incoherent to coherent optical converter. Opt. Eng. **24** (1985) 124–131
[4] Holler F, Tiziani H: A spatial light modulator using BSO crystal. Opt. Commun. **58** (1986) 20–24
[5] Lasprilla MC, Agra Amorim A, Tebaldi M, Bolognini N: Self-imaging through incoherent to coherent conversion. Opt. Eng. **35** (1996) 1440–1445
[6] Tebaldi M, Lasprilla MC, Bolognini N: Analysis of birefringence encoded images. Optik **110** (1999) 127–136
[7] Liu L, Liu X: Opto-optical switching using field enhancing effect in $Bi_{12}SiO_{20}$. J. Appl. Phys. **72** (1992) 337–343
[8] Vachss F, Hesselink L: Measurement of the electrogyratory and electrooptic effects. Opt. Commun. **62** (1987) 159–167
[9] Gerrad A, Burch JM: Introduction to Matrix Methods in Optics. Chap. 4. John Wiley & Sons, London 1975
[10] Feldman A, Brower W, Horowitz D: Optical activity and Faraday Rotation in Bismuth Oxide Compounds. Appl. Phys. Lett. **16** (1970) 201–202